Adiabatic speedup in cutting a spin chain via zero-area pulse control

Run-Hong He,[1] Rui Wang,[1] Feng-Hua Ren,[2] Li-Cheng Zhang,[1] and Zhao-Ming Wang[1,*]
[1]*College of Physics and Optoelectronic Engineering, Ocean University of China, Qingdao 266100, China*
[2]*College of Information and Control Engineering, Qingdao Technology University, Qingdao 266520, China*

(Received 9 March 2020; revised 19 January 2021; accepted 20 April 2021; published 14 May 2021)

The adiabatic quantum information processing task requires that the evolution of a system must be kept in its instantaneous eigenstate. However, normally the adiabaticity will be ruined due to the interaction between the system and the noisy environment in its long evolution time. Here, in this paper, we show that zero-area pulse control can be used to realize the adiabatic process in a nonadiabatic regime. A concrete example is provided where one spin chain is cut into two chains. The pulse function is applied in the laboratory frame and suitable pulse conditions are obtained numerically. We find that compared with the pulse conditions obtained in the adiabatic frame, the results are similar for low-energy-level systems but tend to deviate when the system's energy level increases. We then obtain the pulse conditions theoretically by writing the control Hamiltonian in the adiabatic frame. It is found that a sequence of pulses with intensities tuned by a time-dependent energy difference is required to guarantee an effective adiabatic speedup.

DOI: 10.1103/PhysRevA.103.052606

I. INTRODUCTION

The adiabatic theorem states that if the Hamiltonian of a system changes slowly enough, the system prepared in a nondegenerate eigenstate will remain in that instantaneous eigenstate [1,2]. The adiabatic theorem shows a wide variety of applications in performing quantum information processing tasks, such as adiabatic quantum state transfer [3–6], the adiabatic quantum algorithm [7,8], and adiabatic quantum computation [9–12]. However, theoretically, the quantum adiabatic process requires an infinite long evolution time. Inevitably, the interaction between the system and the environment will cause transitions from one instantaneous eigenstate to other states [13,14], ruining the adiabaticity. Adiabatic speedup or a shortcut to adiabaticity [15] is then proposed to accelerate the adiabatic process, where the evolution of the system goes along an adiabatic passage in a nonadiabatic regime [16–18]. Methods used to accelerate the adiabatic process mainly include transitionless quantum driving [19–22], invariant-based inverse engineering [23–25], acceleration of the adiabatic passage [26,27], superadiabatic driving [28–30], the fast-forward approach [31,32], Dirac dynamics [33], optimal control [34–36] and its comparison with a shortcut to adiabaticity [37], and classical dissipationless driving [38,39]. Recently, the quantum speed limit in a shortcut to adiabaticity has been investigated. The effects of decoherence [40], the Kibble-Zurek mechanism [41], or the link between the quantum speed limit and energetic cost [42] have been discussed.

A leakage elimination operator (LEO) can be used to counteract leakage from a subspace which encodes one logical qubit, or collection of qubits, into the rest of the Hilbert space [43,44]. Recently, schemes of adiabatic speedup were investigated by adding an LEO Hamiltonian to the system's Hamiltonian [45]. The LEO Hamiltonian can be realized by a sequence of pulses. The pulse conditions have been obtained when the pulse function is constructed in the adiabatic frame or the laboratory frame, respectively. The pulse intensity and period must satisfy certain relations to guarantee an effective adiabatic speedup. These include non-zero-area pulses [46,47] and zero-area pulses [45,48]. For zero-area pulses, they have been used to investigate the quantum dynamics of a two-state system [49–51]. However, for the pulse conditions obtained in the laboratory frame, only a constant system energy difference is considered [12]. For most systems, it might not be easy to design a constant energy difference during the time evolution. Here, we aim at finding zero-area pulse control conditions for a time-dependent energy difference when the pulse function is constructed in the laboratory frame. We use cutting a spin chain as an example, a model used to illustrate the shortcut to adiabaticity via non-zero-area pulses [47], zero-area pulse control [52], or high-fidelity ground-state preparation after a nonadiabatic process [53]. We first find suitable pulse conditions by numerical calculations. Compared with the pulse conditions obtained in the adiabatic frame, we find that the results are similar for a low-level system which is in agreement with the conclusion in Ref. [45], but with an increase of the system energy level, they tend to deviate. We then use a two-parametric pulse function to find a more optimal solution. Then, by writing the Hamiltonian in the adiabatic frame and letting the off-diagonal elements of the propagator be equal to zero, we obtain the pulse conditions for the case when the system energy level is *time dependent*. The pulse intensity needs to be tuned by the time-dependent energy difference for an adiabatic speedup. We believe that although we use cutting a spin chain as an example, this control scheme can be extended to a variety of quantum systems.

*Corresponding author: mingmoon78@126.com

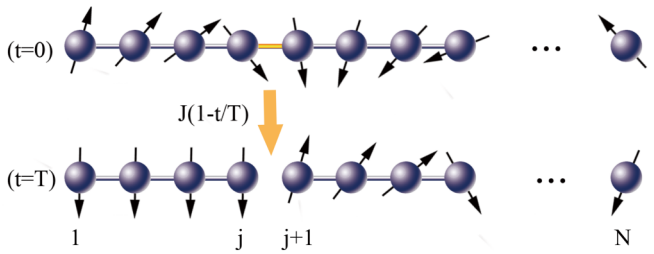

FIG. 1. Schematic illustration of cutting off a one-dimensional spin chain. The nearest-neighbor couplings in the chain are $J=-1$, except that $J_{j,j+1}=J(1-t/T)$ between sites j and $j+1$. The chain will eventually break into two short chains at time $t=T$.

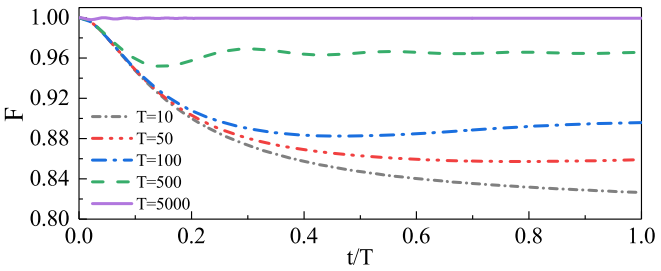

FIG. 2. The fidelity F as a function of the rescaled time t/T for different T. The number of sites $N=45$, and the position to be cut $j=15$.

II. MODEL

We consider a one-dimensional XY spin chain which consists of N spins [47,52–54]. The Hamiltonian of the system can be written as

$$H_0(t)=\sum_{i=1,i\neq j}^{N-1}J_{i,i+1}(X_iX_{i+1}+Y_iY_{i+1}) +J_{j,j+1}(t)(X_jX_{j+1}+Y_jY_{j+1}), \quad (1)$$

where $X_{i(j)}$ and $Y_{i(j)}$ are the Pauli matrices σ_x, σ_y acting on the ith (or jth) site. $J_{i,i+1}$ is the the coupling strength between two nearest-neighbor sites. Suppose the coupling between sites j and $j+1$ changes as

$$J_{j,j+1}=J(1-t/T). \quad (2)$$

For all other couplings we take $J_{i,i+1}=J=-1$, which corresponds to ferromagnetic couplings. This one-dimensional (1D) chain can be realized experimentally by an optical lattice [55,56]. The couplings $J_{j,j+1}$ can be tuned individually by focusing additional laser beams perpendicular to the lattice direction [55–59]. This cutting, for example, can be used to investigate an anomaly in quantum phases induced by borders [60]. From time $t=0$ to $t=T$, one chain has been cut into two chains (see Fig. 1). Suppose initially the system (one chain) is in one of its eigenstates $|E_n(t=0)\rangle$. Our target is then to drive this system to the state $|E_n(t=T)\rangle$.

For the time-dependent Hamiltonian $H_0(t)$ in Eq. (1), the instantaneous eigenstates $|E_n(t)\rangle$ and the corresponding eigenvalues $E_n(t)$ can be represented by

$$H_0(t)|E_n(t)\rangle=E_n(t)|E_n(t)\rangle. \quad (3)$$

At any particular instance these eigenstates constitute an orthonormal set $\langle E_m(t)|E_n(t)\rangle=\delta_{mn}$. They provide a general solution to the time-dependent Schrödinger equation $id|\Psi(t)\rangle/dt=H_0(t)|\Psi(t)\rangle$. We take $\hbar=1$ throughout this paper.

To describe the adiabaticity, we define the fidelity $F(t)\equiv|\langle E_n(t)|\Psi(t)\rangle|$, which measures the closeness of the nth instantaneous eigenstate $|E_n(t)\rangle$ and the evolution state of the system $|\Psi(t)\rangle$. $F(t)\approx 1$ indicates that the system goes along an adiabatic passage.

Due to $[\sum_i Z_i, H_0(t)]=0$, the z component of the total spins is conserved during the time evolution. Here, Z_i represents the Pauli matrix σ_z acting on the ith site. For simplicity, we only consider a single-excited subspace, where the total spins in the z direction is 1. Then for an N-spin chain, it has N eigenstates with N eigenvalues. The analytical solution can be written as [61]

$$|E_n\rangle=\sqrt{\frac{2}{N+1}}\sum_{l=1}^{N}\sin(q_nl)|\mathbf{l}\rangle, \quad (4)$$

where $q_n=\frac{n\pi}{N+1}$, $n=1,2,\ldots,N$. $|\mathbf{l}\rangle$ represents the state with a spin up at the lth site and all other spins down.

Suppose initially the system is at the lowest-energy eigenstate $|E_1(0)\rangle$ in the single-excitation subspace. Now if the system goes along an adiabatic passage $|E_1(t)\rangle$, then $F(t)=|\langle E_1(t)|\Psi(t)\rangle|\approx 1$, where $|E_1(t)\rangle$ is the lowest instantaneous energy eigenstate in the single-excitation subspace of the Hamiltonian $H_0(t)$. $|\Psi(t)\rangle$ is the numerical solution of the time-dependent Schrödinger equation. In Fig. 2 we plot the fidelity $F(t)$ as a function of the rescaled time t/T for different T in cutting a spin chain. As an example, we take the length of the chain $N=45$ and the position to be cut $j=15$. Clearly the fidelity increases with increasing T. When $T>5000$, $F(t)>0.999$ during the evolution. The system enters into an adiabatic regime.

III. DYNAMICAL EVOLUTION UNDER EXTERNAL CONTROL

The time for completing quantum information processing tasks is always required to be as short as possible to avoid dissipation and decoherence [12]. However, adiabatic evolution needs an infinitely long time. An LEO Hamiltonian can be added to the system Hamiltonian to realize the adiabatic speedup. The total Hamiltonian can be written as

$$H(t)=H_0(t)+H_{\mathrm{LEO}}(t), \quad (5)$$

where $H_{\mathrm{LEO}}(t)$ is the LEO Hamiltonian. Physically the LEO Hamiltonian can be implemented by a sequence of pulses. Define the time-dependent bases $|E_n(t)\rangle$ as adiabatic bases and the time-independent bases $|E_n(0)\rangle$ as laboratory bases. Now there are two methods to construct the LEO Hamiltonian. First, it can be constructed as

$$H^a_{\mathrm{LEO}}(t)=c(t)|E_1(t)\rangle\langle E_1(t)|, \quad (6)$$

in the adiabatic frame, where $c(t)$ is the pulse function [8,46]. $|E_1(t)\rangle$ is the lowest-energy eigenstate in the single-excitation subspace [47] or an arbitrary target state [48]. It can also be

constructed as [8,12,46,47]

$$H^e_{\mathrm{LEO}}(t) = c(t)H_0(t), \tag{7}$$

where the pulse function $c(t)$ is added globally on the system Hamiltonian. In this case we say it is constructed in the laboratory frame. Correspondingly, the original system's Hamiltonian $H_0(t)$ can be viewed as in the adiabatic frame for $H^a_{\mathrm{LEO}}(t)$ or the laboratory frame for $H^e_{\mathrm{LEO}}(t)$ if not specified.

Here, we use $H^e_{\mathrm{LEO}}(t)$ to speed up the adiabatic process. Specifically zero-area pulses are used to realize $H^a_{\mathrm{LEO}}(t)$. The Hamiltonian under control now reads

$$H(t) = [1 + c(t)]H_0(t). \tag{8}$$

The zero-area pulse function $c(t)$ can be taken as

$$c(t) = \begin{cases} If(t), & n\tau \leqslant t < (n+1)\tau \quad (n \text{ is even}), \\ -If(t), & n\tau \leqslant t < (n+1)\tau \quad (n \text{ is odd}), \end{cases} \tag{9}$$

where $f(t)$ is an arbitrary non-negative function and I is the amplitude of the pulse intensity. Clearly in a pulse period 2τ, $\int_0^{2\tau} c(t)dt = 0$. For example, when $f(t) = 1$, they are rectangular pulses. When $f(t) = \sin(\omega t)$, they are sine pulses.

To obtain the effective control, the pulse period and intensity must satisfy certain conditions when the LEO Hamiltonians are constructed in the adiabatic frame and the pulse function takes the form as in Eq. (9). The pulse conditions have been explicitly discussed in Refs. [45,62,63]. For example, the conditions are

$$\begin{array}{ll} I\tau = 2k\pi, \quad k = 1, 2, 3, \ldots, & \text{rectangular pulses}, \\ J_0(I\tau/\pi) = 0, & \text{sine pulses}, \end{array} \tag{10}$$

where for sine pulses $J_0(x)$ is the zero-order Bessel function of the first kind. $c(t) = I\sin(\omega t)$ with $\omega\tau = \pi$.

Are the pulse conditions in Eq. (10) still effective for $H^e_{\mathrm{LEO}}(t)$? As an example, we take the rectangular pulses and let $N = 3$, $j = 1$. $T = 1.0$, which is in a nonadiabatic regime. We introduce a parameter $S = \int_0^{\tau} c(t)dt$ to discuss the control effects. Then the pulse conditions are $S = 2\pi k$, $k = 1, 2, 3, \ldots$ for rectangular pulses as in Eq. (10) when the LEO Hamiltonian is added in the adiabatic frame. Figure 3(a) plots the fidelity $F(T)$ as a function of parameter S for different τ. A negative S indicates that the pulse is negative in the first half of the period and vice versa. From Fig. 3(a) it shows similar behavior as in Eq. (10). The fidelity F oscillates with S and for some certain S the fidelity F takes its maximum value. Figures 3(b) and 3(c) plot the fidelity as a function of S for different N, and we take $\tau = T/2$. The results show that with increasing N, there also exists oscillation with respect to

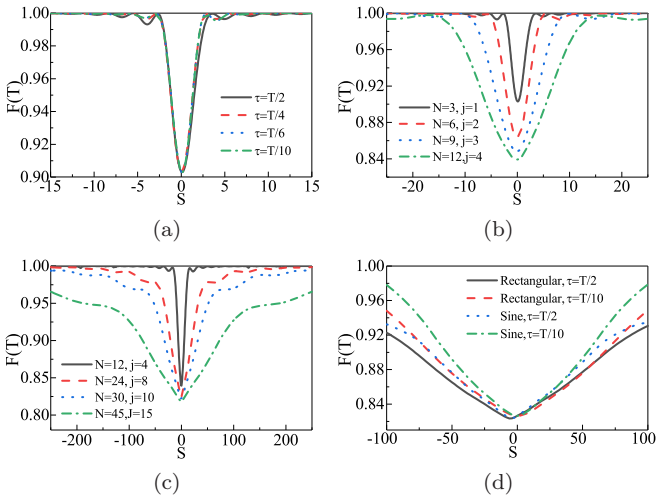

FIG. 3. (a) The fidelity $F(T)$ as a function of the parameter S for different τ. The parameter $S = \int_0^{\tau} c(t)dt$ and it is the integral of $c(t)$ with respect to time in half a pulse period τ. (b) and (c) The fidelity $F(T)$ as a function of different N and j. $T = 1$ in (a)–(c). (d) The fidelity $F(T)$ as a function of the parameter S for rectangular and sine pulses. $T = 10$, $N = 45$, and $j = 15$ in (d).

S. This oscillation behavior becomes weaker for higher-level systems. For example, when $N = 24$ in Fig. 3(c), the oscillation behavior disappears. Compared with Fig. 3(b), a larger S (higher pulse intensity) is required to obtain the adiabatic speedup. This is because in the absence of control the required evolution time T for which the system enters the adiabatic regime increases with increasing N.

In the above discussions, we only consider a rectangular pulse. Now we consider other types of pulses. In Fig. 3(d) we plot the comparison of $F(T)$ as a function of S between rectangular and sine pulses. The parameters $N = 45$, $j = 15$, and $T = 10$ in a nonadiabatic regime. For the sine pulses, $f(t) = \sin(\pi t/\tau)$. Figure 3(d) shows that the fidelity $F(T)$ increases with increasing parameter S in a regime $S \in [-100, 100]$. However, for the same parameter S, the fidelity $F(T)$ of the sine pulses is higher than the rectangular case. Then not only the integral of $c(t)$ but also the details of $c(t)$ determine the control effects. Can we find a way to optimize the pulse function to obtain a higher fidelity? We then introduce a combinatorial function, which is determined by two parameters that mark the weight of each factor in the function. This combinatorial function takes the form

$$c(t) = \begin{cases} -(a_1 + a_2)\frac{2t}{T} + a_1\left(\frac{2t}{T}\right)^2 + a_2\left(\frac{2t}{T}\right)^3, & 0 \leqslant t \leqslant \frac{T}{2}, \\ -(a_1 + a_2)\frac{2t-2T}{T} - a_1\left(\frac{2t-2T}{T}\right)^2 + a_2\left(\frac{2t-2T}{T}\right)^3, & \frac{T}{2} < t \leqslant T. \end{cases} \tag{11}$$

Now for a fixed S, the parameters a_1 and a_2 can be tuned to obtain the maximum fidelity $F(T)$. a_1 and a_2 are taken in the regime $[-100, 100]$. Figure 4 plots the fidelity $F(T)$ as a function of S for different pulses. For the optimal pulse, the maximum fidelity $F(T)$ is obtained in the parameter space of a_1 and a_2. $N = 45$, $J_{15,16} = J(1 - t/T)$, $\tau = T/2 = 5$. From Fig. 4, when $|S|$ is smaller than 85, the fidelity $F(T)$ of the optimal control is higher than the other two cases. However, when $|S| > 85$, the control effects of the optimal pulse cannot be kept. The reason is that we limit the range of parameters a_1 and a_2 in the interval $[-100, 100]$. We conjecture that it might obtain a better result if we extend the range of parameters.

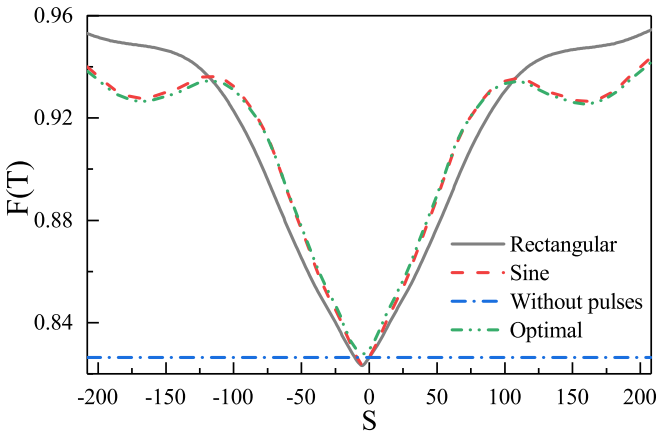

FIG. 4. The fidelity $F(T)$ as a function of the parameter S for different types of pulses. For the optimal pulse, the maximum fidelity $F(T)$ is obtained in the parameter space of a_1 and a_2. $\tau = T/2 = 5$, $N = 45$, and $j = 15$.

Then for a zero-area control pulse, even if the integral of the pulse control in the time domain S is the same, the detail of the function $c(t)$ can be optimally chosen to obtain a higher fidelity. Clearly for the same S, the highest $F(T)$ is obtained for the optimal pulse control. The lowest is obtained for the rectangular pulses and the sine pulses is in the middle.

Now we compare the pulse conditions for two different cases $H^a_{\rm LEO}(t)$ and $H^e_{\rm LEO}(t)$. The parameter S corresponding to the maximum fidelity (first peak and second peak in Fig. 3) as a function of the site number N is plotted in Fig. 5. Clearly for small N, the value of S is similar and with increasing N, they begin to deviate from each other. This result is in agreement with Ref. [45], where a counterunitary transformation from the adiabatic frame to the laboratory frame [47] can be applied to $H^a_{\rm LEO}(t)$, and gives the form of the Hamiltonian in the laboratory frame. For a two-level system, $H^a_{\rm LEO}(t)$ is equivalent to $H^e_{\rm LEO}(t)$ [47]. It does not apply to a high-level system and it might be difficult to realize $H^e_{\rm LEO}(t)$ in an actual experiment. A simple rectangular control function in the adiabatic frame might correspond to a very complex function in the laboratory

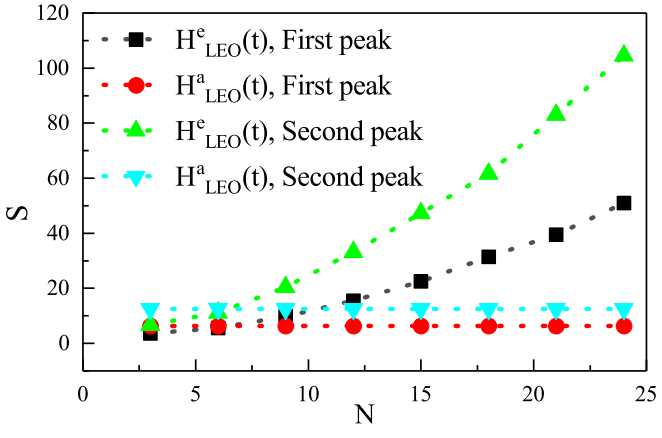

FIG. 5. The parameter S corresponding to the first and second maximum fidelity $F(S)$ as a function of the length N (N energy level) under zero-area rectangular pulses. $T = 1$, $j = N/3$, $\tau = T/2$.

frame for a three-level system [45]. We point out that in Ref. [52], the pulse conditions have been obtained by numerical calculations in cutting a closed spin chain. However, in this paper, we have found that by using a combinatorial function, optimal pulse conditions can be obtained. Furthermore, we will derive an analytical result for the pulse conditions next.

In the above discussions, we have numerically found a sequence of optimal zero-area pulses by numerical calculations. Now we theoretically analyze the corresponding pulse control conditions. First, we write the Hamiltonian $H(t)$ in Eq. (8) in adiabatic bases $|E_n(t)\rangle$. The matrix elements of the Hamiltonian read

$$H_{mn}(t) = -i\langle E_m(t)|\dot{E}_n(t)\rangle \exp(-iC_{nm}(t)), \tag{12}$$

where $C_{nm}(t) = \int_0^t E_{nm}(s)[1 + c(s)]ds$ and $E_{nm}(t) = E_n(t) - E_m(t)$ is the energy difference between the energy levels n and m. The off-diagonal matrix elements will cause transitions between different energy levels and consequently destroy the adiabaticity. The control pulses are then used to reduce the off-diagonal terms. Now we consider the propagator from time $t = 0$ to $t = \delta t$, with $\delta t \ll 1$ and $C(t) \gg 1$. Keeping the first order of the Magnus expansion, $U(\delta t) = \mathcal{T}\exp[-i\int_0^{\delta t} H(t)dt] \approx 1 - i\int_0^{\delta t} H(t)dt$ [12]. Here, $\mathcal{T}$ denotes the time-ordering operator. When $\delta t = \tau \leqslant T$, $\int_0^\tau H_{mn}(s)ds = -i\int_0^\tau \langle E_m(s)|\dot{E}_n(s)\rangle \exp(-iC_{mn}s)ds$. Supposing the control intensity $I \gg 1$, then $\langle E_m(s)|\dot{E}_n(s)\rangle$ varies slowly compared with $\exp[-iC_{mn}(s)]$ and the integrals will be $-i\langle E_m(s)|\dot{E}_n(s)\rangle \int_0^\tau \exp(-iC_{mn}s)ds$ [48]. Clearly the off-diagonal terms in $U(\delta t)$ equal zero when $\int_0^\tau \exp(-iC_{mn}s)ds = 0$. Then the pulse control conditions will be

$$\int_0^\tau c(s)E_{mn}(s)ds = 2\pi k, \quad k = \pm 1, \pm 2, \ldots. \tag{13}$$

In this case, the transition between energy levels n and m is restrained. Supposing the pulse intensity is time dependent, $c(t) = I(t) = \pm I_0/E_{mn}(t)$, then the pulse control conditions are simplified as $I_0\tau = 2\pi k$, which is in accordance with the constant energy difference $E_{mn} = \text{const}$ [12]. Note that from Eq. (13) the positive or negative pulses have the same effects. We then use two consecutive pulses (zero-area pulses) which take positive and negative values, respectively. This case is equivalent to the case where all the negative pulses become positive or vice versa [48]. In our paper, our task is to keep the system in the state $|E_1(t)\rangle$ and the pulse is designed to restrain the transitions from $|E_1(t)\rangle$ to $|E_m(t)\rangle$ with $m \neq 1$. However, by numerical simulations we find that the transition to $|E_2(t)\rangle$ dominates. Then the pulse function is taken as

$$c(t) = I_0/E_{21}(t). \tag{14}$$

In Fig. 6 we plot the fidelity as a function of the rescaled time for four cases: free evolution, which is represented by blue dashed line; with control ($k = 1$), the sky blue solid line; with control ($k = 2$), the red dotted line; and with control ($k = 0.5$), the orange dotted dashed line. For cases $k = 1$ and $k = 2$, the pulses we used satisfy the control conditions in Eqs. (13) and (14). It is worth noting that the pulse control conditions are not met when $k = 0.5$. The total evolution time $T = \pi/3$, which is in a nonadiabatic regime as shown in Fig. 6 for free evolution. The number of sites $N = 10$, and

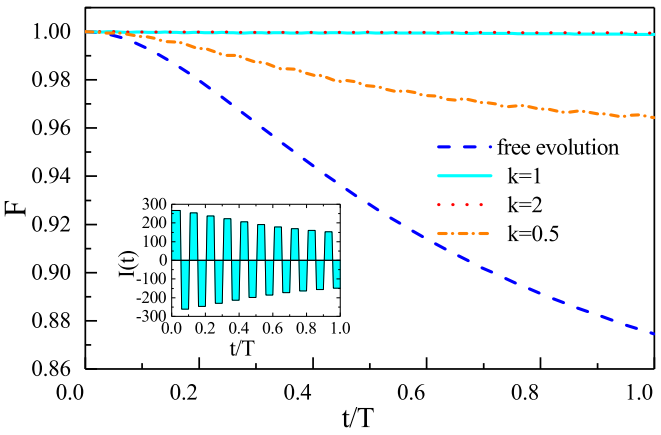

FIG. 6. The fidelity vs the rescaled time t/T for four cases: free evolution; with control $k = 1, 2, 0.5$. For $k = 1, 2$, the pulse conditions are satisfied while $k = 0.5$ does not satisfy.

the position to be cut $j = 3$. The pulse parameters are taken as $I_0 = 2\pi k/\tau$, $\tau = T/20$. The calculation results support the theoretical prediction. Once the pulse control conditions are satisfied, an effective adiabatic speedup can be realized. As an example, at the lower-left-hand corner in Fig. 6 we plot the pulses we applied: I vs t/T for the case $k = 1$. Clearly, the profile of the pulse intensity is tuned by a time-dependent energy difference. The pulse area is almost zero in one period (two consecutive positive and negative pulses).

Dynamical decoupling control [64] can be used to control a dynamical process, where the pulse intensity is strong and the pulse duration is short. For our pulse, the pulse intensity and duration are finite and tunable. Experimentally, time-dependent intensity-modulated [65] continuous dynamical decoupling has been realized to overcome decoherence against fluctuations in a dense ensemble of a nitrogen-vacancy center in diamond. The additional Hamiltonian $[c(t)H_0(t)]$ can be generated by a time-dependent modulation of the amplitude of the original driving.

IV. CONCLUSIONS

The adiabatic quantum information processing task always requires that the evolution time is as short as possible due to the existence of the environment. Adiabatic speedup allows one to drive a system along an adiabatic passage in a nonadiabatic regime. In this paper, we investigate the adiabatic speedup via a zero-area pulse control scheme. While most works consider the control function in the adiabatic frame, we discuss the control function in the laboratory frame. We use cutting a one-dimensional spin chain as an example to discuss the adiabatic process. We compare the pulse conditions between the adiabatic frame and the laboratory frame. It shows that the conditions are similar in low-level systems. With an increasing level of the system, they are inclined to deviate from each other. We consider different types of pulses and find that using the method of superimposing functions of different weights, an optimal pulse with a given evolution time and integral can be obtained. Furthermore, we obtain the pulse control conditions when the LEO Hamiltonian is constructed in the laboratory frame and the energy differences of the system are time dependent. The calculation results show that a tuned pulse intensity is required to obtain an effective adiabatic speedup.

ACKNOWLEDGMENTS

This work was supported by the National Natural Science Foundation of China (Grant No. 11475160), and the Natural Science Foundation of Shandong Province (Grant No. ZR2014AM023).

[1] M. Born and V. Fock, Z. Phys. **51**, 165 (1928).
[2] A. Messiah, *Quantum Mechanics*, Vols. 1 and 2 (Dover, New York, 1964).
[3] V. Balachandran and J. Gong, Phys. Rev. A **77**, 012303 (2008).
[4] J. Gong and P. Brumer, Phys. Rev. A **75**, 032331 (2007).
[5] V. Srinivasa, J. Levy, and C. S. Hellberg, Phys. Rev. B **76**, 094411 (2007).
[6] U. Farooq, A. Bayat, S. Mancini, and S. Bose, Phys. Rev. B **91**, 134303 (2015).
[7] E. Farhi, J. Goldstone, S. Gutmann, J. Lapan, A. Lundgren, and D. Preda, Science **292**, 472 (2001).
[8] H. Wang and L. A. Wu, Sci. Rep. **6**, 22307 (2016).
[9] A. M. Childs, E. Farhi, and J. Preskill, Phys. Rev. A **65**, 012322 (2001).
[10] M. S. Sarandy and D. A. Lidar, Phys. Rev. Lett. **95**, 250503 (2005).
[11] P. Zanardi and M. Rasetti, Phys. Lett. A **264**, 94 (1999).
[12] P. Pyshkin, D.-W. Luo, J. Jing, J. You, and L.-A. Wu, Sci. Rep. **6**, 37781 (2016).
[13] H.-P. Breuer and F. Petruccione, *The Theory of Open Quantum Systems* (Oxford University Press, Oxford, U.K., 2002).
[14] Z.-M. Wang, D.-W. Luo, M. S. Byrd, L.-A. Wu, T. Yu, and B. Shao, Phys. Rev. A **98**, 062118 (2018).
[15] D. Guéry-Odelin, A. Ruschhaupt, A. Kiely, E. Torrontegui, S. Martínez-Garaot, and J. G. Muga, Rev. Mod. Phys. **91**, 045001 (2019).
[16] K. Bergmann, H. Theuer, and B. Shore, Rev. Mod. Phys. **70**, 1003 (1998).
[17] P. Král, I. Thanopulos, and M. Shapiro, Rev. Mod. Phys. **79**, 53 (2007).
[18] D. Guéry-Odelin and J. G. Muga, Phys. Rev. A **90**, 063425 (2014).
[19] M. V. Berry, J. Phys. A: Math. Theor. **42**, 365303 (2009).
[20] M. Demirplak and S. A. Rice, J. Phys. Chem. A **107**, 9937 (2003).
[21] M. Demirplak and S. A. Rice, J. Phys. Chem. B **109**, 6838 (2005).
[22] S. Ibáñez, S. Martínez-Garaot, X. Chen, E. Torrontegui, and J. G. Muga, Phys. Rev. A **84**, 023415 (2011).

[23] H. R. Lewis, Jr. and W. Riesenfeld, J. Math. Phys. **10**, 1458 (1969).
[24] X.-C. Gao, J.-B. Xu, and T.-Z. Qian, Phys. Rev. A **44**, 7016 (1991).
[25] M. Lohe, J. Phys. A: Math. Theor. **42**, 035307 (2008).
[26] S. Guérin, S. Thomas, and H. R. Jauslin, Phys. Rev. A **65**, 023409 (2002).
[27] D. Daems, S. Guérin, and N. J. Cerf, Phys. Rev. A **78**, 042322 (2008).
[28] M. G. Bason, M. Viteau, N. Malossi, P. Huillery, E. Arimondo, D. Ciampini, R. Fazio, V. Giovannetti, R. Mannella, and O. Morsch, Nat. Phys. **8**, 147 (2012).
[29] F.-q. Dou, J. Liu, and L.-b. Fu, Europhys. Lett. **116**, 60014 (2017).
[30] S. Deng, A. Chenu, P. Diao, F. Li, S. Yu, I. Coulamy, A. Del Campo, and H. Wu, Sci. Adv. **4**, 5909 (2018).
[31] S. Masuda and K. Nakamura, Phys. Rev. A **84**, 043434 (2011).
[32] E. Torrontegui, S. Martínez-Garaot, A. Ruschhaupt, and J. G. Muga, Phys. Rev. A **86**, 013601 (2012).
[33] S. Deffner, New J. Phys. **18**, 012001 (2015).
[34] N. Wu, A. Nanduri, and H. Rabitz, Phys. Rev. B **91**, 041115(R) (2015).
[35] L. Van Damme, Q. Ansel, S. J. Glaser, and D. Sugny, Phys. Rev. A **95**, 063403 (2017).
[36] G. Dridi, K. Liu, and S. Guérin, Phys. Rev. Lett. **125**, 250403 (2020).
[37] V. Martikyan, D. Guéry-Odelin, and D. Sugny, Phys. Rev. A **101**, 013423 (2020).
[38] C. Jarzynski, Phys. Rev. A **88**, 040101(R) (2013).
[39] A. Patra and C. Jarzynski, J. Phys. Chem. B **121**, 3403 (2017).
[40] T.-N. Xu, J. Li, T. Busch, X. Chen, and T. Fogarty, Phys. Rev. Research **2**, 023125 (2020).
[41] R. Puebla, S. Deffner, and S. Campbell, Phys. Rev. Research **2**, 032020 (2020).
[42] S. Campbell and S. Deffner, Phys. Rev. Lett. **118**, 100601 (2017).
[43] L.-A. Wu, M. S. Byrd, and D. A. Lidar, Phys. Rev. Lett. **89**, 127901 (2002).
[44] M. S. Byrd, D. A. Lidar, L.-A. Wu, and P. Zanardi, Phys. Rev. A **71**, 052301 (2005).
[45] Z.-M. Wang, M. S. Byrd, J. Jing, and L.-A. Wu, Phys. Rev. A **97**, 062312 (2018).
[46] J. Jing, L. A. Wu, T. Yu, J. Q. You, Z. M. Wang, and L. Garcia, Phys. Rev. A **89**, 032110 (2014).
[47] F.-H. Ren, Z.-M. Wang, and Y.-J. Gu, Phys. Lett. A **381**, 70 (2017).
[48] Z. M. Wang, M. S. Sarandy, and L. A. Wu, Phys. Rev. A **102**, 022601 (2020).
[49] G. S. Vasilev and N. V. Vitanov, Phys. Rev. A **73**, 023416 (2006).
[50] J. M. S. Lehto and K.-A. Suominen, Time-dependent two-level models and zero-area pulse, Phys. Scr. **91**, 013005 (2016).
[51] H.-g. Lee, Y. Song, H. Kim, H. Jo, and J. Ahn, Phys. Rev. A **93**, 023423 (2016).
[52] R. Wang, F.-H. Ren, Y.-J. Gu, and Z.-M. Wang, Quantum Inf. Process. **19**, 1 (2020).
[53] P. Pyshkin, E. Y. Sherman, J. You, and L.-A. Wu, New J. Phys. **20**, 105006 (2018).
[54] P. Pyshkin, E. Y. Sherman, and L.-A. Wu, Acta Phys. Pol., A **135**, 1198 (2019).
[55] Z. M. Wang, L. A. Wu, M. Modugno, M. S. Byrd, T. Yu, and J. Q. You, Phys. Rev. A **89**, 042326 (2014).
[56] V. Boyer, R. M. Godun, G. Smirne, D. Cassettari, C. M. Chandrashekar, A. B. Deb, Z. J. Laczik, and C. J. Foot, Phys. Rev. A **73**, 031402(R) (2006).
[57] C. Becker, S. Stellmer, P. Soltan-Panahi, S. Dörscher, M. Baumert, E. M. Richter, J. Kronjäger, K. Bongs, and K. Sengstock, Nat. Phys. **4**, 496 (2008).
[58] K. Henderson, C. Ryu, C. MacCormick, and M. G. Boshier, New J. Phys. **11**, 043030 (2009).
[59] Z.-M. Wang, C. A. Bishop, J. Jing, Y.-J. Gu, C. Garcia, and L.-A. Wu, Phys. Rev. A **93**, 062338 (2016).
[60] J. Jing, M. Guidry, and L. A. Wu, Sci. Rep. **10**, 2045 (2020).
[61] Z.-M. Wang, C. A. Bishop, M. S. Byrd, B. Shao, and J. Zou, Phys. Rev. A **80**, 022330 (2009).
[62] L.-C. Zhang, F.-H. Ren, Y.-F. Chen, R.-H. He, Y.-J. Gu, and Z.-M. Wang, Europhys. Lett. **125**, 10010 (2019).
[63] Y.-F. Chen, L.-C. Zhang, Y.-J. Gu, and Z.-M. Wang, Phys. Lett. A **382**, 2795 (2018).
[64] C. D. Aiello, M. Hirose, and P. Cappellaro, Nat. Commun. **4**, 1419 (2013).
[65] J. M. Cai, B. Naydenov, R. Pfeiffer, L. P. Mcguinness, K. D. Jahnke, F. Jelezko, M. B. Plenio, and A. Retzker, New J. Phys. **14**, 113023 (2012).